



# Automatic Velocity Picking in the Semblance Domain for a Complete Seismic Profile, Stack and Migration

Wildney W. S. Vieira, Lourenildo W. B. Leite and Boris Sibiryakov, UFPA, Brazil

Copyright 2013, SBGF - Sociedade Brasileira de Geofísica.

This paper was prepared for presentation at the 13<sup>th</sup> International Congress of the Brazilian Geophysical Society, held in Rio de Janeiro, Brazil, August 26-29, 2013.

Contents of this paper were reviewed by the Technical Committee of the 13<sup>th</sup> International Congress of The Brazilian Geophysical Society and do not necessarily represent any position of the SBGF, its officers or members. Electronic reproduction or storage of any part of this paper for commercial purposes without the written consent of The Brazilian Geophysical Society is prohibited.

## Abstract

The specific goal of this work is to present a complete velocity map obtained by an automatic method of velocity picking in the Semblance domain as a sequential nonlinear optimization problem. The steps of the conventional velocity analysis for each common-mid-point section in defined in the following way: first, normal-moveout stacking velocities are estimated by means of Semblance function  $S$ , with the sums along hyperbolic time trajectories producing a map of  $S(v_{rms}, t_0)$ ; second, manual picking is performed on the Semblance map for specific stacking time  $t_0$ ; third, interval velocities,  $v_{int}$ , are calculated based on the picked smooth velocities,  $v_{rms}$ , to construct earth velocity time models.

The present work is multi-task as: (1) to diminish the picking step by considering that stacking velocities are based on an interval velocity model; (2) to search for an interval velocity model that best explains the estimated stacking velocities; and (3) the search is automatic, but subject to geological, physical and mathematical constraints, and editing.

## Introduction

The geological medium is seismically represented by a structure composed of a geometrical form, and a rock (formation) velocity distribution of under overload pressure. A major aim is to determine both components of this structure as a blind inversion process, and for this several velocity types of are described in the literature, as in Al-Chalabi (1974). Imaging the earth's interior is the object of migration, as described by many authors as Etgen et al. (2009), where the velocity distribution is a central issue.

Interval velocity,  $v_{int}$ , the velocity between to sequential reflections, has been a major aim in velocity analysis (VA), since it would be directly related to the geological formation, rock properties, stack, and migration, as described by Buland et al. (2011) and, classically, by Claerbout (1985) and Gazdag and Sguazzerro (1984).

Another important application of measured  $v_p$  and  $v_s$  velocities is to calculate the distribution of density and pressure in the subsurface (Sibiryakov et al., 2013).

Many velocity functions in space-time are defined

to represent the underground aiming the geological knowledge, and among them, the relationship between interval velocity,  $v_{int}$ , and stack velocity,  $v_s$ , play an important role in conventional velocity analysis (CVA). A primary goal in seismic data processing is the determination of both these velocities, and, in CVA,  $v_{int}$  is calculated from the normal moveout velocities related to a Semblance map using a mathematical model as, for example, the Durbaum-Dix type, by considering that  $v_s$  represents the root-mean-square velocity,  $v_{rms}$ , (Hubral and Krey, 1980).

The classical drawback of the Semblance manual peak-picking is that a visual interpretation of the map is necessary, it is based on amplitude and velocity windows, and this can be done for all common-mid-points sections (CMPs). The present study is to propose form a partial to complete elimination of manual peak-picking step, by setting up a model driven strategy. Therefore, VA methods without manual picking stand as an interesting academic study problem.

The restrictions of the present development can be stated as: (1st) limited to 1-D model; (2nd) use of the Durbaum-Dix model for the relation between  $v_{int}$  and  $v_{rms}$ ; (3rd) it does not take into account lateral variations; and (4th) the structural dips are not taken into account in the CMP families (Koren and Ravve, 2006).

## Method

CVA is performed by manual picking of points to construct a curve of velocity versus time in the Semblance domain, and sequentially for each individual CMP to cover the entire seismic section. But, this task carries a strong subjective decision, and it is present in the free and professional seismic software. The result of this operation is a time-distance map of seismic velocity,  $v_s(t_0)$  based on CMP families  $v_s(t_0, x_{CMP})$ . This map can be used directly for NMO correction, stack and time migration, and it can extended to depth migration after the transformation  $v_{rms} \leftrightarrow v_{int}$ , as a first approximation model for the underground depth-and-time interval velocity (Vieira, 2011).

The aim is the solution and implementation of a velocity analysis as a non-linear optimization problem under a priori information and constraints, as a possibility for diminishing the direct subjective participation of the Semblance map interpretation. The result of the optimization process are the root-mean square velocity,  $v_{rms}$ , and interval velocity  $v_{int}$ .

Toldi (1989) has presented this problem and also an original solution, that we denominate as Automatic Velocity Analysis (AVA). Also, the common-reflection-surface (CRS) method, as described by Mann (2002) and

Muller (1999), has a characteristic that is an automatic search in the Semblance domain for the stack velocity, and for single and multiple parameters. The basic reference for the implementation of our optimization procedure was based on Press et al. (2002), and the process steps are shown in Figure 1.

The Semblance function is characterized as being positive and multimodal. Besides this difficulty, the inversion is classified as an ill-posed problem. Therefore, the optimization needs a priori information and constraints, that could be implicit and explicit, for its solution. The a priori information is here defined as an initial velocity model function, the explicit constraints defined as a parameter taper window, and the implicit constraints limited to the control parameter values of the model function.

Due to the ill-posed condition, we organized the optimization problem in the Semblance domain based on two methods: (1) A Global Search using the Simplex method; and (2) a Local Search based on the Conjugate Gradient method. The principle was that with a Global Controlled Multiparametric Unconstrained algorithm we can search for a “global” solution, and with a derivative Local method we can search for statistical details.

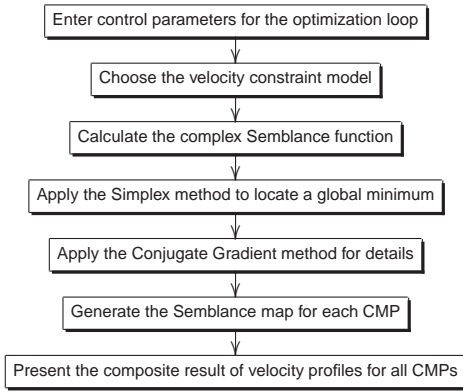


Figure 1: Flowchart of the optimization process for each CMP along the line.

The function object of minimization is the Semblance function, in real form  $S(v_s; t_0)$ , or in complex form  $\psi(v_s; t_0)$ , where the independent variable velocity is  $v_s$  for a fixed time  $t_0$ . For this description, we follow mainly the work of Bernabini et al. (1987).

### Real Coherency Functionals

The normalized Semblance,  $S(v_s; t_0)$ , measures the degree of fitting of amplitudes,  $\bar{u}$ , of the traces of a CMP family for a certain stack velocity, from a first,  $x = x_F$ , to a last,  $x = x_L$ , offset with  $N_x$  points, in a temporal window  $\delta t$ , for a certain reflector  $n$ , marked by the time  $t_0 = t_0^{(n)}$ , and referenced to a point  $P_0(x_0, t_0)$ :

$$S(v_s; t_0) = \frac{\left\{ \frac{1}{N_t} \sum_{t=t_0-\delta t/2}^{t_0+\delta t/2} \frac{1}{N_x} \sum_{x=x_F}^{x_L} \bar{u}[t(x; t_0, v_s)] \right\}^2}{\frac{1}{N_t} \sum_{t=t_0-\delta t/2}^{t_0+\delta t/2} \frac{1}{N_x} \sum_{x=x_F}^{x_L} \left\{ \bar{u}[t(x; t_0, v_s)] \right\}^2}. \quad (1)$$

$S(v_s; t_0)$  admits values in the interval  $[0, 1]$  irrespective of

the signal amplitude, and it quantifies the signal polarity uniformity throughout the traces of the corrected NMO family amplitudes  $\bar{u}[t(x; t_0, v_s)]$ . The quantity  $S(v_s; t_0)$  is proportional to the energy ratio between numerator and denominator of equation (1). In the NMO correction and stack, the function  $S(v_s; t_0)$  can also be interpreted as a function to be optimized, from where results the optimum value of  $v_s$ , where  $t(x; t_0, v_s)$  is given by:

$$t(x; t_0, v_s) = \sqrt{t_0^2 + \frac{x^2}{v_s^2}}. \quad (2)$$

Other  $t(x; t_0)$  trajectories are known for different stack techniques, as in Mann (2002) for the CRS stack.

In the above equations (1) and (2), the quantity  $v_s$  can interpreted as the stack velocity. The zero offset stack section is also interpreted as the Normal Incidence (Reflection) section. Later, in the sequel, the quantity  $v_s$  will be interpreted as the root-mean-square velocity  $V_{rms}$ , and related to the interval velocity  $v_{int}$ .

### Complex Coherency Functionals

The coherency functional used for the case of complex-valued function is the adapted analytical signal written as:

$$\psi(v_s; t_0) = S(v_s; t_0) + i H_S(v_s; t_0); \quad (3)$$

where  $S(v_s; t_0)$  is real-valued, and  $H_S(v_s; t_0)$  is obtained from  $S(v_s; t_0)$  by application of the Hilbert transform,  $\mathbf{H}$ , with respect to the  $v_s$  variable of the  $S(v_s; t_0)$  function. In the frequency domain we write that:

$$H_S(v_s; t_0) = \mathbf{H}\{S(v_s; t_0)\} = \mathbf{F}^{-1}\{i \text{Sgn}(\omega) S(\omega; t_0)\}, \quad (4)$$

where  $\mathbf{F}$  represent the direct, and  $\mathbf{F}^{-1}$  the inverse Fourier transform,  $i$  is the imaginary unit,  $\omega$  is the angular frequency with respect to  $v_s$ , and  $\text{Sgn}(\omega)$  is the sign function in the frequency domain. The Semblance functional,  $S$ , generalizes to  $\mathcal{S}$  as:

$$\mathcal{S}(v, t_0) = \frac{\sum_{t=t_0-\delta t/2}^{t_0+\delta t/2} \left| \frac{1}{N_x} \sum_{x=x_0}^X \psi(x, t; v) \right|^2}{\sum_{t=t_0-\delta t/2}^{t_0+\delta t/2} \frac{1}{N_x} \sum_{x=x_0}^X |\psi(x, t; v)|^2}, \quad (5)$$

where the vertical bars denote the moduli of the complex function involved and, if it operates on complex-valued  $\psi$  function, the quantity  $\mathcal{S}$  is still a real-valued coherency function. In the present case we have defined  $|\psi(v_s; t_0)|$  as:

$$|\psi| = \sqrt{\text{Real}^2(\psi) + \text{Imag}^2(\psi)}. \quad (6)$$

### Simplex Method

The classical Simplex is adapted to our problem by making the Semblance optimization object function. The Simplex is often referenced to Nelder and Mead (1965), and it is classified as a random controlled global search method, and as being a direct search method, it does not carry statistical operator relations.

The Simplex is based on four basic operations: reflection, expansion, contraction and reduction in the parameter

space,  $\mathbf{m}$ . It is admitted that  $\mathbf{m}_i^{(k)}$  be the  $i$ -th vertex of a polyhedron in the  $\mathbf{m}$  space, and in the  $k$ -th optimization iteration. The correspondent value of the object function of minimization is called  $f(\mathbf{m}_i^{(k)})$ , and after each iteration the stop criterion is evaluated as, for instance, by the  $\chi$  function given in the form:

$$\chi(\mathbf{m}; t_0) = \sqrt{\frac{1}{n+1} \sum_{i=1}^{n+1} [S(\mathbf{m}_i^{(k)}; t_0) - S(\mathbf{c}^{(k)}; t_0)]^2} \leq \varepsilon, \quad (7)$$

that is the square root average of the deviations between  $S(\mathbf{m}_i^{(k)}; t_0)$  and  $S(\mathbf{c}^{(k)}; t_0)$  calculated with respect to the vertices of the centroid  $\mathbf{c}^k$ , and  $\varepsilon$  a small positive number used as the stop criterion. The parameter space is defined as  $\mathbf{m} = \mathbf{v}_s$ .

### Conjugate Gradient Method

The Gradient Method (GM) is defined as a Derivative Local Search Method. As such, its application is rather severe for obtaining plausible results due to the multimodal characteristic of the object function of minimization, and the is obtained solution will depend on a priori and constraint information. The Conjugate Gradient is a specific technique of the GMs, described in many textbooks as by Fletcher (2001), and we follow Press et al. (2002) for the computer program implementation.

The object function of minimization is defined as equation (1), where the model function,  $t(x; t_0, v_s)$ , is given by equation (2), with  $v_s = v_{rms}$  and  $v_{int}$  given by equations (8) and (9):

$$v_{rms,n} = \sqrt{\frac{\sum_{i=1}^n v_{int,i}^2 \Delta t_i}{\sum_{i=1}^n \Delta t_i}} \rightarrow v_{rms}(t) = \sqrt{\frac{1}{t} \int_0^t v_{int}^2(\tau) d\tau}, \quad (8)$$

$$v_{int,n} = \sqrt{\frac{t_{n+1} v_{rms,n+1}^2 - t_n v_{rms,n}^2}{t_{n+1} - t_n}} \rightarrow v_{int}(t) = \sqrt{\frac{d}{dt} t v_{rms}^2(t)}. \quad (9)$$

These equations are Durbaum-Dix transform referenced to a  $n$ -th layer, or a  $n$ -th reflector, or a  $n$ -th interval velocity  $v_{int,n}$ , or a  $n$ -th  $v_{rms,n}$  velocity, and for the condition of zero offset.

Equations (8) and (9) are rewritten in discrete (nonuniform intervals  $\Delta t_i$ ) and continuous forms for interpretation of their effects. In the continuous forms, the traveltime  $t$  participates as a decaying factor in the calculus of  $v_{rms}(t)$ , and as an amplification in the calculus of  $v_{int}(t)$ .

The transformation to depth of the micro-interval velocity,  $v_{int,n} \leftrightarrow v(z_n)$ , is calculated by equation:

$$z_n = z_{n-1} + \frac{1}{2} v_{int,n} [t_n - t_{n-1}]. \quad (10)$$

A first observation with respect to the above discrete pair is that the process is over the  $\Delta t$  micro-intervals, establishing a continuous calculation, without observing the interval between two consecutive natural reflections. Therefore, the effective source pulse should be a natural smoothing operator. The length of the source pulse can be, for instance, up to 10 points.

A second observation is that  $v_{rms}$  is an integral average value of the subsurface velocity sampled by the traveling wave, therefore it must appear as a smooth function.

The third observation is that  $v_{int}$  has the form of a derivative of the squared  $v_{rms}$  function, what makes  $v_{int}$  very sensitive to noise present in  $v_{rms}$ . As a consequence, the calculus of this derivative needs to be edited for unreal jumps in a form of one more constraint to the process, and we have included in the algorithm to detect jumps in  $v_{int,n}$  over a highest velocity allowed,  $v_{high} = 5000\text{m/s}$ , and to proceed with a  $N_S$  point smoothing operator, for instance  $N_S = 5$ , depending on the analysis for the effective source pulse made in the section.

### Results and Conclusions

The obtained results are presented by the following sequence of figures taken as examples: CMP sections, Semblance interpretation sections, composite velocity maps, stack, and migration.

The data used for the present test is the Marmousoft seismic project. (Versteeg and Grau, 1991).

An important point in the present optimization process is the constraint model adopted, where the constraints were imposed to the  $v_{int}$  function. The process sweeps from left-to-right across the the profile in a controlled form, where some CMPs are used to initiate the loop process. In the present example, we chose the first CMP (number 95) to start the process, and ran across the profile up to the last CMP (number 515), using only CMP with maximum coverage. The total number of CMPs in the profile is 616.

One velocity function option implemented is described by Ravve and Koren (2006a) and Ravve and Koren (2006b), used to represent  $v_{rms}(z)$  and  $v_{rms}(t)$ . The  $v_{rms}(z)$  is given by:

$$v_{rms}(z) = v_0 + \Delta v [1 - e^{-\frac{k_a}{\Delta v} z}]. \quad (11)$$

$\Delta v = v_\infty - v_a$ , where  $v_\infty$  is the asymptotic velocity as  $z \rightarrow \infty$ , and  $v_a(x, y)$  is the local velocity at the reference point, and  $k_a$  the gradient for the exponential decay. The  $v_{rms}(t)$  counterpart, with  $t$  one-way traveltime is given by:

$$v_{rms}(t) = \frac{v_a v_\infty}{v_a + \Delta v e^{-\frac{k_a v_\infty}{\Delta v} t}} \quad (12)$$

One common observation is that the semblance map can be interpreted as a linear-by-parts function. Therefore, for the present examples, the constraint model adopted is described by:

$$v_{rms}(t_i) = v_0 + k_{t,i} t_i, \quad (i = 1, N_s), \quad (13)$$

where  $N_s$  is the number of segments, usually 4 or 5, and  $k_{t,i}$  the respective segment gradient. We call attention to the fact that the corners between the  $(i)$  segments of the  $v_{rms}$  function is a source of jumps in the  $v_{int}(t_i)$  function.

Implicit constraints are applied during the Global Search with the Simplex method on the interval velocities ( $v_{int}$ ), in order to limit the random search around a "global" minimum. In the sequence of the process, the Gradient is applied for the solution detail. Also, explicit constraints are applied in the Global search in order to fix the solution around considered known velocity values as, for instance, the top weathering and water layers.

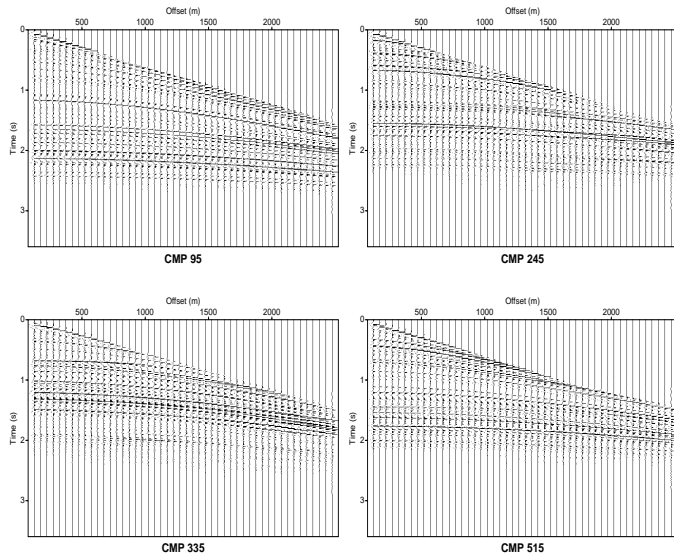


Figure 2: Selected CMPs where the reflection hyperbolic forms are clear.

Figure 2 shows the contents of CMP sections, where is clear the “hyperbolic” reflection forms necessary to satisfy the theoretical model.

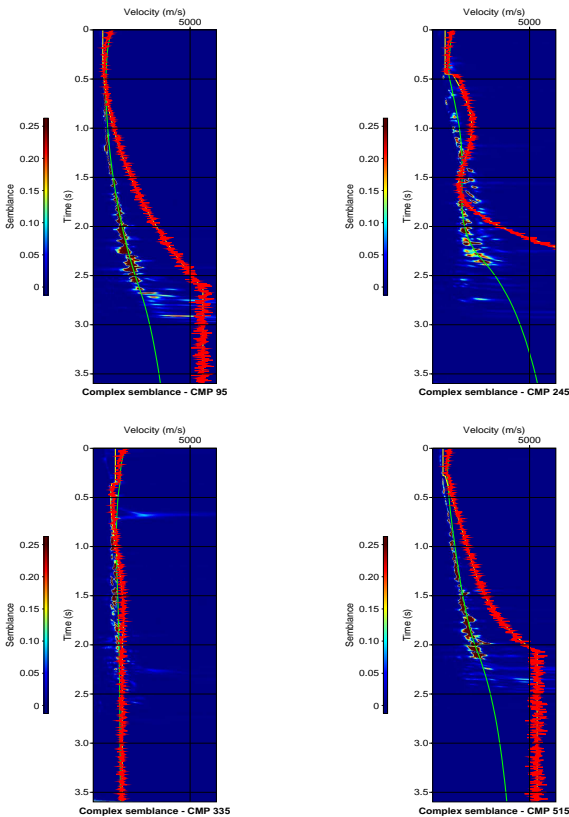
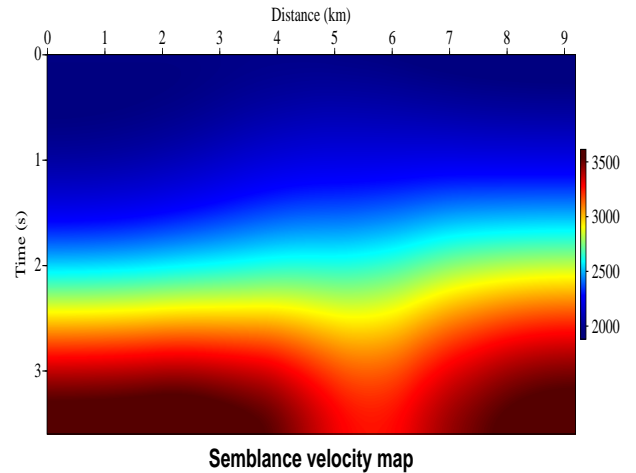


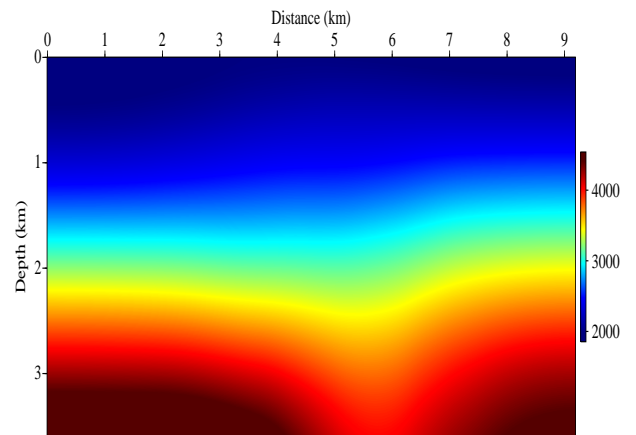
Figure 3: Semblance maps of the selected CMPs. The green lines show the  $v_{rms}$ , the yellow lines the  $v_{int}$ , and the red lines the Simplex explicit constraints on  $v_{int}$  for the automatic picking.

Figure 3 shows the automatic interpretations plotted over the Semblance maps corresponding to Figure 2. The maps show clearly the multi-valued characteristics of the Semblance function, object of minimization, and consequently the necessity for strong constraints and a priori information. The green line indicate the  $v_{rms}$  velocity, the yellow line the  $v_{int}$  velocity, and the red line the random constraint imposed to the  $v_{int}$  velocity for the global search. The top and bottom of the Semblance maps show details of the velocity constraints imposed with a constant value and with a gradient, respectively. Model constraints should to imposed be attend a geologically plausible solution.



Semblance velocity map

(a) Time,  $v_{rms}(t, x_{CMP})$ .



Semblance based depth velocity distribution

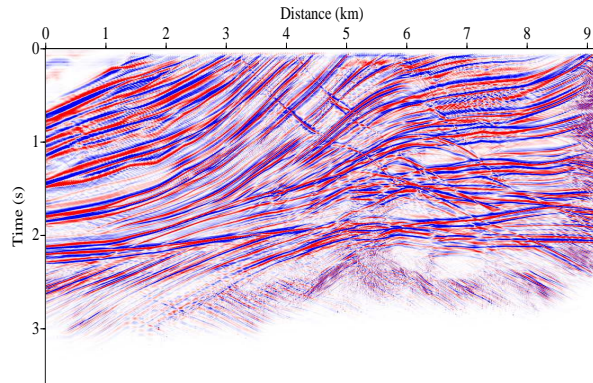
(b) Depth,  $v_{int}(z, x_{CMP})$ .

Figure 4: Semblance velocity maps obtained by the automatic process:  $v_{rms} \leftrightarrow v_{int}$ .

Figure 4(a) presents the automatic time velocity models, used on Figure 5(a) of the conventional stack, and on Figure 5(b) for the Kirchhoff poststack time migration.

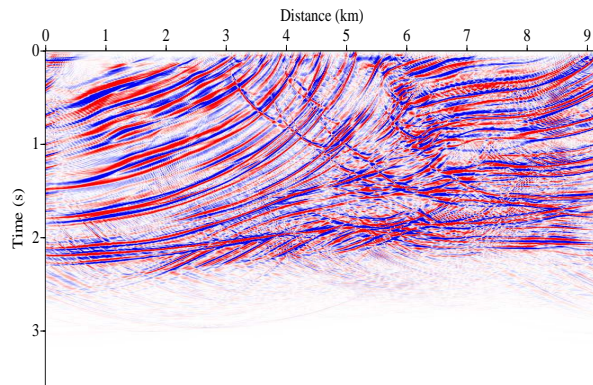
Figure 5(c) was obtained using the velocity model of Figure 4(b), and it was selected because it shows consistent

results with the automatic semblance velocity models transformed to depth.



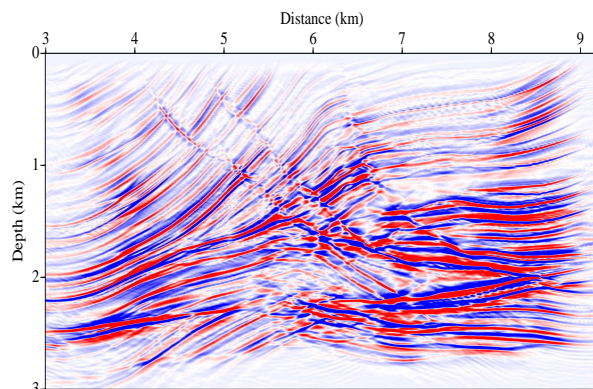
Conventional NMO stack

(a) Stack.



Kirchhoff migration

(b) Time migration.



Kirchhoff migration

(c) Depth migration.

Figure 5: Conventional NMO stack, Kirchhoff time migration and Kirchhoff depth migration. AGC gain was applied with a window length of 0.5s to reveal weak events. The velocity model used was of Figure 4.

As a first conclusion, the constraints on the interval velocities should be strong, that means narrow band around the expected value of  $v_{\text{int}}(t, x_{\text{CMP}})$ . The general nonlinear optimization model constraints are fundamental for a geologically plausible solution, since the Semblance function show to be clearly multi-valued, and consequently the necessity for a priori information.

Even though, the  $v_{\text{rms}}(t, x_{\text{CMP}})$  function is smooth, the  $v_{\text{int}}$  function is very sensitive and give unreal jumps for small variations of  $v_{\text{rms}}$ , as shown in Figures 3, and there is necessity of a jump detection and smoothing operators.

The depth migration were selected as final reference conventional procedures, and not on the bases of physical-geological analysis, for comparing the consistency of the obtained velocity models.

## References

- Al-Chalabi, M., 1974, An analysis of stacking, rms, average and interval velocities over a horizontally layered ground: *Geophysical Prospecting*, **22**, 458–475.
- Bernabini, M., Carrion, P., Jacovitti, G., Rocca, F., Treitel, S., and Worthington, M. H., 1987, *Deconvolution and inversion*: Blackwell Scientific Publications.
- Buland, A., Kolbjørnsen, O., and Carter, A. J., 2011, Bayesian dix inversion: *Geophysics*, **76**, no. 2, 759–775.
- Claerbout, J., 1985, *Imaging the earth's interior*: Blackwell Scientific Publications.
- Etgen, J., Gray, S. H., and Zhang, Y., 2009, An overview of depth imaging in exploration geophysics: *Geophysics*, **74**, no. 6, WCA5–WCA17.
- Fletcher, R., 2001, *Practical methods of optimization*: John Wiley and Sons.
- Gazdag, J., and Sguazzerro, P., 1984, Interval velocity analysis by wave extrapolation: *Geophysical Prospecting*, **32**, 454–479.
- Hubral, P., and Krey, T., 1980, Interval velocities from seismic reflection time measurements: *Society of Exploration Geophysicists*.
- Koren, Z., and Ravve, I., 2006, Constrained dix inversion: *Geophysics*, **7**, no. 6, 113–130.
- Mann, J., 2002, *Extensions and applications of the common-reflection-surface stack method*: Ph.D. thesis, Universitat Fridericana Karlsruhe.
- Muller, T., 1999, *The common reflection surface stack - seismic imaging without explicit knowledge of the velocity model*: Ph.D. thesis, Universitat Fridericana Karlsruhe.
- Nelder, J. A., and Mead, R., 1965, A simplex method for function minimization: *The Computer Journal*, **7**, 308–313.
- Press, W. H., Teukolsky, A., Vetterking, W. T., and Flannery, B. P., 2002, *Numerical recipes in fortran 90*: Cambridge University Press.

- Ravve, I., and Koren, Z., 2006a, Exponential asymptotically bounded velocity model: Part i - effective models and velocity transformations: *Geophysics*, **71**, no. 3, T53–T65.
- Ravve, I., and Koren, Z., 2006b, Exponential asymptotically bounded velocity model: Part ii - ray tracing: *Geophysics*, **71**, no. 3, T67–T85.
- Sibiryakov, B. P., Leite, L. W. B., and Vieira, W. W. S., 2013, Model of structured continuum and relation between specific surface, porosity and permeability: Thirteenth International Congress of The Brazilian Geophysical Society.
- Toldi, L. T., 1989, Velocity analysis without picking: *Geophysics*, **54**, no. 2, 191–199.
- Versteeg, R. J., and Grau, G., 1991, The marmousi experience: EAGE.
- Vieira, W. W. S., 2011, Análise de velocidade por otimização do semblance na reflexão sísmica: Master's thesis, Universidade Federal do Pará.

### **Acknowledgments**

The authors would like to thank the Brazilian institutions UFPA (*Universidade Federal do Pará*), FINEP (*Financiadora de Estudos e Projetos*), ANP (*Agência Nacional do Petróleo*) and PETROBRAS (*Petróleo Brasileiro S/A*) for the research support, and in special to the National Institute of Science and Technology (*Instituto Nacional de Ciência e tecnologia*), INCT-GP, do MCT/CNPq/FINEP. The thanks are also extended to CAPES for the scholarship.

The thanks are also extended to The Project Science Without Borders.